Eur. Phys. J. D **1**, 223-226 (1998)

THE EUROPEAN PHYSICAL JOURNAL D

A model for second harmonic generation in poled glasses

A. Le Calvez, E. Freysz[a], and A. Ducasse

Centre de Physique Moléculaire Optique et Hertzienne, Université de Bordeaux I, 351, cours de la libération, 33405 Talence, France

Received: 21 August 1997 / Accepted: 20 November 1997

Abstract. The microscopic description of the poling process allows us to describe the occurrence of second-order nonlinear susceptibilities in thermally poled glasses. At high temperature and during poling, the ionic impurities move towards the electrodes to screen the applied voltage. The high electric field appearing at both interfaces of the sample can reorient polar and highly nonlinear moieties and induce a second-order susceptibility. After poling, the reoriented molecules and induced charge distribution are frozen. The latter creates a static permanent electric field which may result in an electric field-induced second-order nonlinearity. This model makes it possible to optimize the induced nonlinearities.

PACS. 42.70.Ce Glasses, quartz – 42.65.Ky Harmonic generation, frequency conversion – 42.81.Dp Propagation, scattering, and losses; solitons

Myers *et al.* [1] have observed with a Second Harmonic Generation (SHG) experiment that large second order nonlinearity ($\chi^{(2)} \sim 1$ pm/V) can be produced in poled fused silica. This phenomenon has been evidenced in many different glasses [2,3] and has attracted much interest because of the new possibilities offered in monolithically integrated nonlinear devices. Two mechanisms, *i.e.* frozen-in electric field E_0 ($\chi^{(2)}_{\rm eff} = \chi^{(3)}E_0$) and oriented dipoles ($\chi^{(2)}_{\rm d}$), have been assumed to explain this induced nonlinearity [1,4,5]. It has been suggested that migration of ionic impurities is responsible for the permanent electric field E_0 [1,4]. However, the proposed interpretations cannot explain all experimental observations such as the nonlinearity location, poling time, temperature dependence, *etc.* Up to now, no model describing these two mechanisms and taking into account the microscopic characteristics of the glass has been available. Therefore, the optimization of the induced $\chi^{(2)}$ is difficult. Here, we present a microscopic model of the poling process based on the migration of ionic impurities. Our analysis, which is in good agreement with most of the experimental observations, accounts for both mechanisms $\chi^{(2)}_{\rm eff} = \chi^{(3)}E_0$ and $\chi^{(2)}_{\rm d}$.

To model the poling process, the glass is assimilated to a neutral "solid electrolyte" containing anions and cations of respective concentrations $N_0/z_{\rm a}$, $N_0/z_{\rm c}$ and charges $-z_{\rm a}e$, $z_{\rm c}e$. These ions which are mainly due to ionic impurities or defects are mobile at high temperatures and under high applied electric fields. Since the dimensions of the electrodes are usually large compared to the glass thickness L, the problem will be considered in unidimensional terms along the x coordinate where x stands for the direction of the applied electric field. During the poling process, an electric voltage V_0 is applied between the cathode and the anode respectively located at $x = 0$ and $x = L$. The evolution of the ion concentrations is then described by a system of coupled equations containing the equations of diffusion for the different ionic species and Laplace's equation. Moreover, to take into account the solid nature of the glass, we will assume that only a finite number of sites, respectively labeled $N_{\rm cm}$ and $N_{\rm am}$ for the cations and the anions, is able to receive these ions. $N_{\rm c}(x)$ and $N_{\rm a}(x)$ are respectively the cation and anion concentrations at the abscissa x. Then, if we assume that only two ionic species of charge $-z_{\rm a}e$ and $z_{\rm c}e$ are involved, the system of coupled equations becomes [6,8]:

$$\begin{cases} \dfrac{\partial N_{\rm c}(x)}{\partial t} = -\dfrac{\partial J_{\rm c}(x)}{\partial x} \\ \qquad = u_{\rm c}N_{\rm c}(x)\dfrac{\partial^2 V(x)}{\partial x^2} \\ \qquad\quad + D_{\rm c}\dfrac{N_{\rm cm}}{N_{\rm cm} - N_{\rm c}(x)}\dfrac{\partial^2 N_{\rm c}(x)}{\partial x^2} \\ \dfrac{\partial N_{\rm a}(x)}{\partial t} = -\dfrac{\partial J_{\rm a}(x)}{\partial x} \\ \qquad = -u_{\rm a}N_{\rm a}(x)\dfrac{\partial^2 V(x)}{\partial x^2} \\ \qquad\quad + D_{\rm a}\dfrac{N_{\rm am}}{N_{\rm am} - N_{\rm a}(x)}\dfrac{\partial^2 N_{\rm a}(x)}{\partial x^2} \\ \dfrac{\partial^2 V(x)}{\partial x^2} = -[z_{\rm c}N_{\rm c}(x) - z_{\rm a}N_{\rm a}(x)]\dfrac{e}{\varepsilon} \end{cases} \quad (1)$$

In the set of equations (1), $V(x)$ is the electric potential, ε is the glass dielectric constant while $J_{\rm c}(x)$ and $J_{\rm a}(x)$ are the cation and anion fluxes at the abscissa x. The

[a] e-mail: freysz@frbdx11.cribx1.u-bordeaux.fr

constants u_i and D_i (i = c or a) are respectively the mobility and the diffusion constant of the associated ion. These two quantities are related by the Einstein law: $u_i = D_i|z_i|e/kT$ where k is the Boltzmann constant and T the temperature. To solve the set of equations (1) in the steady state, six boundary conditions are necessary. The first is given by $V(L) - V(0) = V_0$. The second comes from the Gauss theorem: $(\mathrm{d}V/\mathrm{d}x)_{x=0} = (\mathrm{d}V/\mathrm{d}x)_{x=L}$. For blocking electrodes and in the absence of chemical reactions at the electrodes, we must have: $J_{\mathrm{c,a}}(0) = J_{\mathrm{c,a}}(L) = 0$. In fused silica, at about 300 °C, it is mainly sodium ions (Na^+) ($z_\mathrm{c} = 1$) which are mobile [9]. Therefore, the anions will be assumed to be immobile so that $N_\mathrm{a}(x) = N_\mathrm{am} = N_0$ if $z_\mathrm{a} = 1$. The set of equations (1) can be solved numerically. However, further simplifications of this equation allowing an analytical resolution can be made by noticing that $eV_0/kT \gg 1$ under usual poling conditions ($T \approx 300$ °C, $V_0 \approx 3$ kV). Indeed, in these conditions, the expression of the potential is:

$$\begin{cases} V(0 < x < d_1) = -[\sqrt{-V(0)} - \sqrt{(N_\mathrm{cm} - N_0)e/2\varepsilon}\, x]^2 \\ V(d_1 < x < L - d_2) = 0 \\ V(L - d_2 < x < L) = [\sqrt{V(L)} - \sqrt{N_0 e/2\varepsilon}\,(L - x)]^2 \end{cases} \quad (2)$$

$V(0)$ and $V(L)$ are obtained from the boundary conditions: $V(0) = -V_0 N_0/N_\mathrm{cm}$ and $V(L) = V_0(1 - N_0/N_\mathrm{cm})$. d_1 and d_2 are the distances over which the applied electric field is screened at the cathode and the anode respectively: $d_1 = \sqrt{-2\varepsilon V(0)/(N_\mathrm{cm} - N_0)e}$ and $d_2 = \sqrt{2\varepsilon V(L)/N_0 e}$. In Figure 1, we have plotted the potential $V(x)$, the charge distribution $\rho(x) = [z_\mathrm{c}N_\mathrm{c}(x) - z_\mathrm{a}N_\mathrm{a}(x)]e$ and the associated electric field $E(x) = -\mathrm{d}V(x)/\mathrm{d}x$ for a typical silica sample poled under usual conditions. The numerical and analytical results are presented and are in good agreement. The macroscopic charge migration is responsible for the screening of the electric potential in the bulk of the glass. Notice that the screening distances d_1 and d_2 are much smaller than the sample thickness $L \sim 1$ mm, and that $d_2/d_1 \sim N_\mathrm{cm}/N_0$. In consequence, the electric field $E(x) \sim V_0/d_2 \sim 10^8$ V/m at the glass interfaces is very high. The asymmetry between the anodic and cathodic sides results from the assumed immobility of the anions. Indeed, to screen the applied voltage, a large cationic depletion is created close to the anode. As the number N_cm of available sites is high, these cations concentrate strongly at the cathode. It is important to notice that the temperature T has disappeared from the expressions of $V(x)$, of d_1 and d_2, so T does not seem to play any role in the steady-state regime. However, SHG experiments on poled glasses have shown that no signal can be detected if the poling temperature T is lower than 150 °C. In fact, the importance of T becomes apparent in the study of the transient regime. Again, since $eV_0/kT \gg 1$ under usual poling conditions, the resolution of the set of equations (1) is simplified. Thus, by applying the Von Hippel *et al.* method [10], one obtains the time $\tau(T)$ necessary to reach the steady state:

$$\tau(T) = d_2 LkT/eV_0 D_\mathrm{c} = d_2 LkT/eV_0 D_0 \exp[E_\mathrm{a}^{\mathrm{Na}^+}/kT]$$

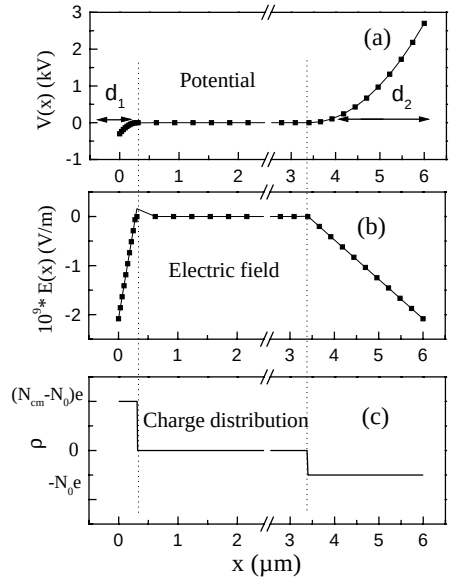

Fig. 1. Profiles of the potential $V(x)$ (a), of the electric field $E(x)$ (b) and of the charge distribution $\rho(x)$ (c) in a sample at high temperature (T = 300 °C) and under high voltage (V_0 = 3 kV). The glass is assumed to contain N_0 = 3 ppm of Na^+ ions and a number of available sites $N_\mathrm{cm} = 10\ N_0$. The continuous line and the points stand for the analytical and numerical results respectively. Figure 1c is not to scale.

where the diffusion constant D_c is equal to

$$D_\mathrm{c} = D_0 \exp[-E_\mathrm{a}/kT]$$

with $D_0 = 0.37$ cm^{2}s^{-1}, and $E_\mathrm{a}^{\mathrm{Na}^+}$ the activation energy for Na^+ in fused silica is equal to 1.12 eV [9]. This time is strongly dependent on the temperature: for example, τ(25 °C) $\sim$ 15 000 years while τ(300 °C) $\sim$ 1 minute when $V_0 \sim 3$ kV, $L \sim 5$ mm, $N_0 \sim 3$ ppm. These values of τ show why a temperature of at least 150 °C is necessary to pole a glass. Myers *et al.* measured the time τ *versus* the poling temperature and indeed found an Arrhenius law with an activation energy of 1.3 eV close to $E_\mathrm{a}^{\mathrm{Na}^+}$ [4]. Therefore, temperature may be seen up to now as being only a kinetic parameter of the poling problem but with no influence on the amplitude of the electric field created. The same conclusion is valid for the sample thickness L.

Since during poling the electric field $E(x)$ is non-null only close to the interfaces over distances d_1 at the cathode and d_2 at the anode (Fig. 1b), any reorientation by this field of the dipoles of eventual hyperpolarizable entities could occur only in these regions. Therefore, the existence of the mechanism $\chi_\mathrm{d}^{(2)}$ should be characterized by a location of the SH signal at the sample interfaces. The susceptibility $\chi_\mathrm{d}^{(2)}$ induced by reorientation of the dipoles can be estimated by considering a long molecule with ξ along the molecular axis and by neglecting the environmental interactions [11]. The poling symmetry implies that only

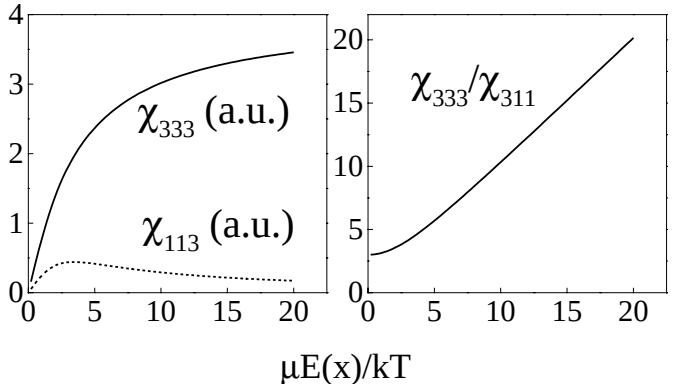

Fig. 2. Evolution of the $\chi^{(2)}$ tensor elements $\chi^{(2)}_{333}$ and $\chi^{(2)}_{311}$ and of the ratio $R_\chi = \chi^{(2)}_{333}/\chi^{(2)}_{311}$ when $\mu E(x)/kT$ increases.

two elements of the tensor $\chi^{(2)}$ ($\chi^{(2)}_{\rm d}$ or $\chi^{(2)}_{\rm eff}$) are non-null and independent: $\chi^{(2)}_{333}$ and $\chi^{(2)}_{311}$ (where axis 3 is parallel to the poling direction). The elements of $\chi^{(2)}_{\rm d}$ are then:

$$\begin{cases} \chi^{(2)}_{\rm d\ 311} = & N\beta^{(2)}_{\xi\xi\xi}[(a^2+3) - 3a/{\rm th}(a)]/a^3 \\ \chi^{(2)}_{\rm d\ 333} = & N\beta^{(2)}_{\xi\xi\xi}[a(6+a^2)/{\rm th}(a) - 3(2+a^2)]/a^3 \end{cases} \quad (3)$$

where N is the number of hyperpolarizable molecules per unit volume, $\beta^{(2)}_{\xi\xi\xi}$ is the dominant molecular susceptibility, $a(x) = \mu E(x)/kT$ with μ the dipole moment of the hyperpolarizable entities present in the glass and $E(x)$ the electric field in the sample during poling. The relationship (3) shows that the ratio $a(x)$ between the dipolar interaction and thermal energies is an important parameter. In Figure 2, we have plotted the evolution of $\chi^{(2)}_{\rm d\ 333}$ and $\chi^{(2)}_{\rm d\ 311}$ as a function of $a(x)$. Their behaviors for high $a(x)$ values are explained by a complete reorientation of the dipoles along axis 3. Therefore, the ratio $R_\chi = \chi^{(2)}_{333}/\chi^{(2)}_{311}$ increases from 3 up to high values when $a(x)$ increases. Notice that the highest values of $\chi^{(2)}_{\rm d\ 333}$ are obtained at low temperatures where the poling times are unfortunately excessively long. In consequence, for a given poling duration, an optimal value of the temperature exists. This phenomenon has been observed by different authors [2,12].

It is now important to try to identify such reoriented moieties. It is difficult to consider at such a temperature that SiO_2 entities totally linked by covalent bounds can be reoriented. However, other processes related to local rearrangement of defects are possible. It is interesting to notice that an increase in the induced nonlinearity related to defects has been observed after X-ray irradiation of synthetic silica [13]. These defects are characterized by a dipole moment, a second order molecular susceptibility and an activation energy. During poling at high temperature, similar defects could undergo a local electrically biased relaxation which could induce a biased reorientation. Therefore, they would be rearranged in a non-centrosymmetric manner and could contribute to the induced nonlinearity.

Once the steady state is reached, the second step of the poling process consists in decreasing the temperature and removing the applied voltage. Then, the oriented dipoles and the induced $\chi^{(2)}_{\rm d}$ nonlinearity are quenched. Similarly, the charge distribution $\rho(x)$ (Fig. 1c) is frozen and the sample can be assimilated to a charged capacitor. The induced permanent electrostatic field $E_0(x)$ can be determined by using the Gauss theorem:

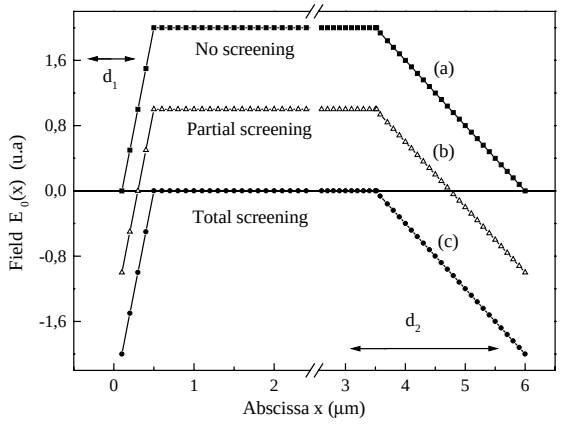

Fig. 3. Distribution of the frozen-in space electric field $E_0(x)$ for a sample poled under the same conditions as in Figure 1. The three curves correspond to three different screening rates: (a) none, (b) partial and (c) total screenings.

$$\begin{cases} E_0(0 < x < d_1) = A_0\ x/d_1 \\ E_0(d_1 < x < L - d_2) = A_0 \\ E_0(L - d_2 < x < L) = A_0\{1 - [x - (L - d_2)]/d_2\} \end{cases} \quad (4)$$

where $A_0 = N_0 d_2 e/\varepsilon$. The profile of $E_0(x)$ is plotted in Figure 3a. However, the induced electrostatic distribution $\rho(x)$ (Fig. 1c) is unstable in ambient air. Indeed, the charges displaced during the poling procedure towards the sample interfaces may be screened by charges present in the air. According to the screening rate, the amplitude of $E_0(x)$ is shifted as illustrated in Figures 3b and 3c. In any respect, the electric field induced is again high ($E_0 \sim V_0/d_2 \sim 10^8$ V/m). As shown in Figure 3, the location in the sample of the induced effective second-order susceptibility $\chi^{(2)}_{\rm eff}(x) = \chi^{(3)}E_0(x)$ depends on the screening rate. For instance, in the absence of screening, this nonlinearity is induced in the bulk of the glass, while for a total screening, only the interfaces over distances d_1 and d_2 contribute to $\chi^{(2)}_{\rm eff}(x)$. An important difference with the reorientational mechanism comes from the value of $R_\chi = \chi^{(2)}_{333}/\chi^{(2)}_{311}$ since, for this mechanism, this ratio is given by $\chi^{(3)}_{3333}/\chi^{(3)}_{3311}$ which is equal to 3 in an isotropic medium [14].

In our model, if a bulk nonlinearity is detected, it must be related to the mechanism $\chi^{(3)}E_0$ without external charge screening. On the contrary, if a surface nonlinearity is observed, it may be due either to the reorientational mechanism $\chi^{(2)}_{\rm d}$ or to a frozen-in space field ($\chi^{(3)}E_0$) screened by external charges. Moreover, in the

case of a surface nonlinearity, an SH signal must be detected on both anodic and cathodic interfaces. However, in an SHG experiment in transmission, the SH signal S_{anode} generated by the anodic region must be much greater than the signal S_{cathode} produced by the cathodic region: $S_{\text{anode}}/S_{\text{cathode}} \sim (d_2/d_1)^2$. The ratio between the $\chi_{\text{d}}^{(2)}$ and $\chi^{(3)}E_0$ contributions is related to the dipolar moment, the hyperpolarizabity of the reoriented moieties and to the third-order susceptibility of the glass. The model makes it possible to evaluate the influence of all parameters (V_0, T, N_0, L, $\cdots$) and to optimize the induced nonlinearity. Our recently performed SHG experiments on fused silica samples confirm our theoretical analysis (Le Calvez *et al.*, to be published). In the present paper, the model have been focused on fused silica but can be easily generalized to other glasses in which both anions and cations can be mobile.

The authors thank the Region Aquitaine and the Direction des Recherches Etudes et Techniques for financial support and G. Couturier (CPMOH Bordeaux) for helpful discussions.

References

1. R.A. Myers, N. Mukherjee, S.R.J. Brueck, Opt. Lett. **16**, 1732 (1991).
2. K. Tanaka, K. Kashima, K. Hirao, N. Soga, A. Mito, H. Nasu, Jpn. J. Appl. Phys. **32**, L843 (1993).
3. H. Nasu, K. Kurachi, A. Mito, H. Okamoto, J. Matusoka, K. Kamiya, J. Non Cryst. Solids **181**, 83 (1995).
4. N. Mukherjee, R.A. Myers, S.R.J. Brueck, J. Opt. Soc. Am. B **11**, 665 (1994).
5. P.G. Kazansky, P.St.J. Russell, Optics Comm. **110**, 611 (1994).
6. L. Landau, E. Lifschitz, *Physique Statistique* (Édition Mir 1967).
7. G. Couturier, Ph. D. thesis, University of Bordeaux I (France), n°726 (1982).
8. A. Le Calvez, Ph. D. Thesis, University of Bordeaux I (France), n°1653, (1997).
9. N.P. Bansal, R.H. Doremus, *Handbook of Glass Properties* (Academic Press, New-York, 1986).
10. A. Von Hippel, E.P. Gross, J. P. Jelatis, M. Geller, Phys. Rev. **91**, 568 (1953).
11. $\chi_{dijk}^{(2)} = N\beta_{\xi\xi\xi}^{(2)} \int_0^{2\pi} \mathrm{d}\varphi \int_0^{\pi} \mathrm{d}\theta \sin\theta G(\theta) b_{i\xi} b_{j\xi} b_{k\xi}$ with $G(\theta) \propto \exp(\mu E(x)\cos\theta/kT)$ where $(b_{i\xi})$ is the transformation matrix relating the molecular and substrate frames.
12. K. Tanaka, A. Narazaki, K. Hirao, N. Soga, J. Non Cryst. Solids **203**, 49 (1996).
13. A. Kameyama, E. Muroi, A. Yokotani, K. Kurosawa, P.R. Herman, J. Opt. Soc. Am. B **14**, 1088 (1997)
14. S. Kielich, IEEE J. Quantum Electron. **QE-5**, 562 (1969).